Molecular theory of smectic-A liquid crystals

L. Mederos* and D. E. Sullivan
Department of Physics and Guelph-Waterloo Program for Graduate Work in Physics, University of Guelph, Guelph, Ontario, Canada N1G 2W1
(Received 28 July 1988)

A generalization of the McMillan-Kobayashi mean-field theory of smectic-A liquid crystals to explicitly include anisotropic hard-core interactions is described. Hard-core effects are incorporated using perturbation arguments on a reference system of aligned parallel ellipsoids with effective shape parameters, which is treated by a nonlocal-density-functional approach. The results reveal the necessity of including both anisotropic repulsions and certain "symmetry-breaking" attractive interactions, usually omitted from McMillan-Kobayashi treatments, for obtaining stable smectic-A phases. The theory shows explicitly how the interlayer distance in a smectic phase results, variationally, from incompressibility of the hard cores. Phase diagrams that include nematic, smectic, as well as isotropic liquid and vapor phases are presented, using both temperature and density (or pressure) as independent variables.

I. INTRODUCTION

Current theories of nematic liquid crystals have stressed the importance of both repulsive and attractive anisotropic intermolecular forces in stabilizing the nematic state.[1,2] The situation regarding smectic phases is less clear. The widely used theory of smectic-A liquid crystals introduced by McMillan[3] and Kobayashi,[4] which is based on mean-field treatment of a model fluid containing only attractive anisotropic interactions, yields many results in qualitative agreement with experiment.[5] On the other hand, recent theoretical works have given evidence that smectic ordering can be induced by purely hard-core interactions in model systems composed of rigid rods.[6–9] With few exceptions,[10–12] the joint effects of hard-core and attractive interactions on smectic behavior have not been studied. The works in Refs. 10–12 are limited by use of a low-density second-virial approximation and either a truncated spherical-harmonic expansion[11,12] or, at the opposite extreme, a square-wave representation[10] of the effective ordering potential due to the hard cores.

In this paper we investigate smectic-A liquid crystals using an approach similar to that of generalized van der Waals theories of bulk[1,2] and inhomogeneous[13,14] nematic liquids. The contributions of anisotropic attractive interactions to the free energy are treated by mean-field approximation, in common with most works referred to above. Hard-core contributions are analyzed using a nonlocal-density functional method developed in the contexts of crystallization and interfaces of simple hard-sphere fluids.[15–17] The extension of this method to anisotropic fluids is based on notions of molecular perturbation theory developed elsewhere[18] as well as on the mapping[19,20] between perfectly aligned hard ellipsoids and hard spheres. The present model has the restriction that anisotropic hard-core interactions alone should not be sufficient to produce smectic phases. Nonetheless, we shall demonstrate the necessity of accounting explicitly for such interactions in the description of these phases. Our work clarifies the significance of several effects that are either omitted or treated in an empirical manner by the classical McMillan[3–5] approach; for example, the variational nature of the interlayer distance (smectic period) and the role of symmetry-breaking terms[11,12,21,22] in the model intermolecular potential. We predict several aspects of the joint influence of temperature and pressure on smectic phase diagrams which are of experimental relevance.

The general theory is presented in Sec. II A. Sec. II B discusses calculational details; in particular, on obtaining numerically exact solutions of the theory in contrast with the more common analyses using *low-order* Fourier series. The application of a Landau expansion of the smectic free energy is described in Sec. II C. Numerical results are given in Sec. III, while Sec. IV concludes with a discussion.

II. THEORY

A. Free-energy functional

A bulk smectic liquid crystal is characterized by a one-particle probability density $\rho(\mathbf{r}\omega)$ that depends on both position $\mathbf{r}$ and orientation ω. This is analogous to a *nonuniform* nematic liquid.[13,14,18] On separating the total intermolecular potential $V(1,2)$ between each pair of molecules into repulsive and attractive parts, where the latter is denoted $V_A(1,2)$, the conventional mean-field approximation to the Helmholtz free energy of such a system is

$$F=F_R+\tfrac{1}{2}\int d1\,d2\,\rho(1)V_A(1,2)\rho(2)\ , \tag{2.1}$$

where i stands for the coordinates $\mathbf{r}_i$ and ω_i, $i=1,2$. Here F_R represents the contributions to the free energy due to repulsive intermolecular forces in addition to ideal-gas effects.

If we retain only the ideal-gas limit of F_R,

$$F_{\rm id}=k_BT\int d1\,\rho(1)[\ln\rho(1)-1]\ , \tag{2.2}$$

where k_B is Boltzmann's constant and T is temperature, then the resulting approximation for F is equivalent

[apart from specifying $V_A(1,2)$, see below] to that of McMillan[3] and Kobayashi.[4] However, there is no basis for neglecting the effects of intermolecular repulsions at liquid densities. For studying interfaces of nematic liquid crystals, Telo da Gama[13] modeled the latter forces by simple *hard-sphere* interactions. In that case, we can write exactly

$$F_R = F_{\rm id} + \Delta F_{\rm HS}[\{\rho(\mathbf{r})\}] , \tag{2.3}$$

where the interaction term $\Delta F_{\rm HS}$ is a functional of the angle-averaged density $\rho(\mathbf{r}) = \int d\omega \rho(\mathbf{r}\omega)$. By appropriate scaling,[19,20] the expression in (2.3) also applies if the repulsive interactions are taken between *perfectly aligned hard ellipsoids*. Arguments given in Ref. 18, based on extending current ideas of molecular perturbation theory[23] to liquid crystals, suggest that incomplete orientational order can be approximately incorporated in the latter picture by considering the shape parameters of the ellipsoids (i.e., major and minor axis diameters) to be functionals of the angular probability distribution.[24] This is a nontrivial extension, however, and in the present work we shall simply investigate a lowest-order model in which the axis diameters have constant "effective" values. We denote the major diameter, parallel to the direction of alignment, and the minor diameter by $\sigma_\parallel$ and $\sigma_\perp$, respectively.

Thus we take F_R to be given by (2.3) using a suitably scaled hard-sphere functional $\Delta F_{\rm HS}$. We shall evaluate the latter using the nonlocal-density-functional theory developed by Tarazona and co-workers,[15–17] which preserves much of the simplicity of a local-density approximation to $\Delta F_{\rm HS}$ (see, e.g., Ref. 13) but remains physically sensible when $\rho(\mathbf{r})$ exhibits significant oscillations over molecular length scales.[25] This expresses $\Delta F_{\rm HS}$ as

$$\Delta F_{\rm HS} = k_B T \int d\mathbf{r} \rho(\mathbf{r}) \Delta\psi_{\rm HS}(\bar\rho(\mathbf{r})) , \tag{2.4}$$

where $k_B T \Delta\psi_{\rm HS}(\bar\rho)$ is the excess hard-sphere free energy per particle in a uniform bulk phase of density $\bar\rho$. Taking account of the mapping between hard spheres and parallel hard ellipsoids,[19,20] the averaged (or "coarse-grained") density $\bar\rho(\mathbf{r})$ in (2.4) is given by

$$\bar\rho(\mathbf{r}) = \int d\mathbf{s}\, w(|\mathbf{s}|;\bar\rho(\mathbf{r})\sigma^3) \rho(\mathbf{r} + \vec\sigma\cdot\mathbf{s}) . \tag{2.5}$$

Here w is a dimensionless weighting function of the dimensionless separation $\mathbf{s}$, and also depends on the reduced density $\bar\rho(\mathbf{r})\sigma^3$ at position $\mathbf{r}$, where the equivalent hard-sphere diameter σ satisfies $\sigma^3 = \sigma_\perp^2 \sigma_\parallel$. The explicit form of w is described in the Appendix. In (2.5), $\vec\sigma$ denotes a diagonal tensor with components $\sigma_\perp$, $\sigma_\perp$, and $\sigma_\parallel$ in the x, y, and z directions, respectively, where the alignment direction is chosen to be parallel to the z axis. We take $\Delta\psi_{\rm HS}(\bar\rho)$ in (2.4) to be given by the quasiexact Carnahan-Starling expression

$$\Delta\psi_{\rm HS}(\bar\rho) = \frac{\xi(4-3\xi)}{(1-\xi)^2}, \quad \xi = \frac{\pi\bar\rho\sigma^3}{6} . \tag{2.6}$$

Returning to the attractive potential $V_A(1,2)$ in (2.1), we shall model that by the form

$$V_A(1,2) = V_1(r_{12}) + V_2(r_{12}) P_2(\cos\theta_{12}) + V_3(r_{12})[P_2(\cos\theta_1') + P_2(\cos\theta_2')] . \tag{2.7}$$

Here $r_{12} = |\mathbf{r}_{12}| \equiv |\mathbf{r}_2 - \mathbf{r}_1|$ is the intermolecular distance, θ_{12} is the angle between the symmetry axes of the molecules, θ_i' is the angle between the axis of molecule i and the intermolecular vector $\mathbf{r}_{12}$, and P_2 denotes the second Legendre polynomial. On omitting the last term, involving $V_3(r_{12})$, (2.7) reduces to the "Maier-Saupe"[26] form used by McMillan[3] and Kobayashi,[4] as well as many others.[5] The limitations of the latter for a realistic description of interactions between mesogenic molecules have been pointed out several times.[12,14,21,22] Indeed, for *weakly* anisotropic nonpolar molecules, the term in $V_3(r_{12})$ provides the dominant angle dependence of the potential,[23] while evidence given in Ref. 18 indicates that the functions $V_2(r_{12})$ and $V_3(r_{12})$ are of comparable magnitude for attractive rod-shaped molecules with elongations typical of mesogens. [We add that contributions to the functions $V_n(r_{12})$ can arise from pure spherically symmetric attractive forces that are cut off inside an angle-dependent core.[1,11,12]] At the level of spherical-harmonic truncation assumed in (2.7), additional angle-dependent terms also arise, as considered, for example, in lattice-model calculations of Ronis and co-workers.[27] These terms appear[18] to have significantly smaller magnitudes than those displayed in (2.7) and hence will be neglected here. The specific forms of the functions $V_n(r)$ used in this work will be introduced later.

The total Helmholtz free energy F of our theory is given by the combination of Eqs. (2.1)–(2.7). For uniform bulk phases, i.e., isotropic and nematic fluids, $\rho(\mathbf{r})$ equals a constant ρ and (2.5) reduces [by normalization of w (Refs. 15 and 16)] to $\bar\rho(\mathbf{r}) = \rho$. The hard-core contribution to the free energy in these cases is identical to that for hard spheres of diameter σ, and the thermodynamics of the model are the same as in Ref. 13. For modulated phases, the hard-core contribution is the same as *if* the system consisted of perfectly aligned hard ellipsoids, although we shall apply the theory under conditions of arbitrary orientational order. In the absence of the attractive potential $V_A(1,2)$, stable smectic phases should not occur in this theory,[20] a point which we shall check in Sec. III.

B. Method of solution

A closed integral equation for the probability density $\rho(\mathbf{r}\omega)$ can be obtained by functional minimization of the free energy derived in Sec. II A. For the case of a bulk smectic-A phase, $\rho(\mathbf{r}\omega) = \rho(z\omega)$ varies only in the z direction, coinciding with the direction of alignment. The integral equation can be expressed as

$$\rho(z\omega) = \frac{\rho_0 \exp -[H(z) + \beta V_{\rm eff}(z\omega)]}{\frac{1}{d}\int_0^d dz \int d\omega \exp -[H(z) + \beta V_{\rm eff}(z\omega)]} , \tag{2.8}$$

where $\beta = (k_B T)^{-1}$, ρ_0 is the mean number density,

$$\frac{1}{d}\int_0^d dz \int d\omega \rho(z\omega) = \rho_0 , \tag{2.9}$$

and d is the smectic period. Here $V_{\rm eff}(z\omega)$ is the effective one-particle potential due to attractive pair interactions,

$$V_{\rm eff}(1)=\int d2\, V_A(1,2)\rho(2)\ , \tag{2.10}$$

while $H(z)$ is a somewhat analogous effective potential resulting from hard-core interactions. Specifically,

$$H(z)=\Delta\psi_{\rm HS}[\bar\rho(z)]+\int dz'\rho(z')\Delta\psi'_{\rm HS}[\bar\rho(z')]\frac{\delta\bar\rho(z')}{\delta\rho(z)}\ , \tag{2.11}$$

where $\Delta\psi'_{\rm HS}(\bar\rho)\equiv d\Delta\psi_{\rm HS}(\bar\rho)/d\bar\rho$. The functional derivative $\delta\bar\rho(z')/\delta\rho(z)$ can be worked out using (2.5) and the results for w described in the Appendix.

Using (2.7) and assuming uniaxial orientational symmetry appropriate for smectic-A phases, the effective potential (2.10) takes the form

$$V_{\rm eff}(z\omega)=I_1(z)+I_2(z)P_2(\cos\theta)\ , \tag{2.12}$$

where θ denotes the polar angle of a molecule with respect to the z axis. The functions $I_1(z)$ and $I_2(z)$ involve convolutions of the potentials $V_n(r)$ with the angle-averaged density $\rho(z)\equiv\int d\omega\,\rho(z\omega)$ and with the orientational order parameter

$$\begin{aligned}\eta(z)&=\int d\omega\,\rho(z\omega)P_2(\cos\theta)\\&=2\pi\int_0^\pi d\theta\sin(\theta)\rho(z,\cos\theta)P_2(\cos\theta)\ .\end{aligned} \tag{2.13}$$

We shall not give the explicit expressions for I_1 and I_2. From (2.8) and (2.10)–(2.12), one can derive a pair of coupled integral equations for $\rho(z)$ and $\eta(z)$ which, in principle, can be solved numerically without further approximation. We have done that in a few cases, although we find it to be simpler and more efficient numerically to obtain solutions of the theory by minimization of the free energy with respect to the Fourier coefficients ρ_m and η_m, using the representations

$$\begin{aligned}\rho(z)&=\rho_0+\sum_{m=1}^{M}\rho_m\cos(mqz)\ ,\\ \eta(z)&=\eta_0+\sum_{m=1}^{M}\eta_m\cos(mqz)\ ,\end{aligned} \tag{2.14}$$

with a suitably large truncation limit M, where $q=2\pi/d$. [The order parameters traditionally denoted[3–5] η, τ, and σ correspond to the present quantities η_0/ρ_0, $\rho_1/(2\rho_0)$, and $\eta_1/(2\rho_0)$, respectively.] In this context, it is convenient to express the free energy per unit volume f as

$$\begin{aligned}f=\frac{k_BT}{d}\int_0^d dz\,\rho(z)[\ln\rho(z)-1+\Delta\psi_{\rm HS}(\bar\rho(z))\\ -S_{\rm rot}(z)]+e_{\rm MF}\ .\end{aligned} \tag{2.15}$$

Here $e_{\rm MF}$ denotes the mean-field internal energy per volume,

$$e_{\rm MF}=\tfrac{1}{2}\int_0^d dz\int d\omega\,\rho(z\omega)V_{\rm eff}(z\omega)\ , \tag{2.16}$$

while $S_{\rm rot}(z)$ denotes the reduced local rotational entropy per particle

$$S_{\rm rot}(z)=-\int d\omega\,\hat f(z\omega)\ln[4\pi\hat f(z\omega)]\ , \tag{2.17}$$

where $\hat f(z\omega)\equiv\rho(z\omega)/\rho(z)$ is the normalized angular distribution function. Using the Fourier series representations (2.14) and the model for $V_A(1,2)$ in (2.7), the internal energy defined in (2.16) becomes

$$\begin{aligned}e_{\rm MF}=&\frac{\tilde V_{10}}{2}\rho_0^2+\frac{\tilde V_{20}}{2}\eta_0^2\\&+\frac{1}{4}\sum_{m=1}^{M}(\tilde V_{1m}\rho_m^2+\tilde V_{2m}\eta_m^2+2\tilde V_{3m}\rho_m\eta_m)\ ,\end{aligned} \tag{2.18}$$

where $\tilde V_{nm}\equiv\tilde V_n(mq)$ denotes appropriate Fourier transforms of the functions $V_n(r)$. For arbitrary wave number q',

$$\tilde V_n(q')=\begin{cases}4\pi\int_0^\infty dr\,r^2V_n(r)j_0(q'r), & n=1,2\\ -4\pi\int_0^\infty dr\,r^2V_3(r)j_2(q'r), & n=3\end{cases} \tag{2.19}$$

where $j_l(q'r)$ are spherical Bessel functions. One sees that $\tilde V_3(q')$ vanishes when $q'=0$, as taken into account in (2.18), which is consistent with the absence of any effect of $V_3(r)$ on the bulk behavior of uniform phases in the present theory.[14] The coarse-grained density $\bar\rho(z)$ in (2.15) can likewise be expressed analytically in terms of the order parameters ρ_m, cf. Appendix.

It can be shown that $S_{\rm rot}(z)$ defined in (2.17) is a universal function of the reduced orientational order parameter

$$\bar\eta(z)\equiv\eta(z)/\rho(z)=\int d\omega\,\hat f(z\omega)P_2(\cos\theta)\ . \tag{2.20}$$

This follows as a consequence of (2.8) and (2.12), which are formally exact outcomes of the present theory. Those equations lead to the form

$$\hat f(z\omega)=\frac{\exp[\Lambda(z)P_2(\cos\theta)]}{\int d\omega\exp[\Lambda(z)P_2(\cos\theta)]}\ . \tag{2.21}$$

At *equilibrium*, $\Lambda(z)$ is identical to the function $-\beta I_2(z)$ introduced in (2.12). However, we can alternatively view (2.20) and (2.21) as defining a 1:1 relation between $\bar\eta(z)$ and $\Lambda(z)$, which establishes the local dependence of $S_{\rm rot}(z)\equiv S_{\rm rot}[\bar\eta(z)]$ on $\bar\eta(z)$. In the following work, we have calculated $S_{\rm rot}(\bar\eta)$ numerically for a large discrete set of points in the allowed range $-\frac{1}{2}<\bar\eta<1$. Cubic spline fitting was then applied to generate a continuous curve $S_{\rm rot}(\bar\eta)$ for use in subsequent calculations.

Given the above considerations and a model for the potentials $V_n(r)$, the free energy (2.15) becomes a function of the variational parameters η_0, η_m, ρ_m ($m=1-M$) *and* d. Apart from some recent works,[6–9,12] most previous theories have ignored the variational nature of the smectic period. After scaling z by d in (2.15), the parameter d appears explicitly in the functions $\tilde V_{nm}$, cf. (2.18) and (2.19), as well as in the Fourier series for the coarse-grained density $\bar\rho(z)$, see (A8) in the Appendix. The integral with respect to z in the first term of (2.15) was eval-

uated numerically using an adaptive Romberg method.[28] At fixed ρ_0 and T, we minimize f with respect to the order parameters and d using a quasi-Newton method[28] (IMSL subroutine ZXMIN). We have used values of M as large as 20, although for many purposes of interest much smaller values are sufficient. First-order phase coexistence boundaries have been calculated by standard double-tangent construction on the equilibrium free energy $f(\rho_0, T)$.

C. Landau expansion

The nematic-smectic phase boundaries predicted by the theory can by approximately (or exactly, when they are second order) determined by a much simpler Landau analysis. This is based on expanding the free energy $f(\rho_1,\rho_2,\ldots;\eta_0,\eta_1,\eta_2\ldots)$ at fixed ρ_0, T, and period d about that of a nematic phase characterized by a nonzero value $\eta_0^{(N)}$ of only the mean orientational order parameter η_0. On eliminating, by minimization of f, all order parameters $\rho_2,\rho_3,\ldots,\eta_0-\eta_0^{(N)},\eta_1,\eta_2,\ldots$, in terms of the fundamental Fourier component ρ_1, the Landau expansion takes the expected form[29]

$$f-f^{(N)}=c_2\rho_1^2+c_4\rho_1^4\cdots\ , \tag{2.22}$$

where $f^{(N)}$ is the free energy of the nematic phase. It has been shown in previous work[30,31] on smectic-A liquid crystals that the coefficient c_2 depends only on coupling between the leading-order Fourier components ρ_1 and η_1, while c_4 depends additionally on coupling to the second-order components ρ_2 and η_2 as well as $\eta_0-\eta_0^{(N)}$. In particular,

$$c_2=\tfrac{1}{2}(f_{\rho_1\rho_1}-f_{\rho_1\eta_1}^2/f_{\eta_1\eta_1})\ , \tag{2.23}$$

where $f_{\phi_i\phi_j}\equiv(\partial^2 f/\partial\phi_i\,\partial\phi_j)$, evaluated in the reference nematic state. We will pass up showing the corresponding expression for c_4, which is considerably more complex.[30,31] The second derivatives of the free energy in (2.23) are found to be given by

$$\begin{aligned} f_{\rho_1\rho_1}&=\frac{k_BT}{2}\left[\frac{1}{\rho_0}-\tilde{c}_{\rm HS}(q^*)\right]+\frac{k_BT\bar{\eta}_0^2}{2\rho_0}\Lambda'(\bar{\eta}_0)\\ &\quad+\tfrac{1}{2}\tilde{V}_{11}\ , \\ f_{\eta_1\eta_1}&=\frac{k_BT}{2\rho_0}\Lambda'(\bar{\eta}_0)+\tfrac{1}{2}\tilde{V}_{21}\ , \\ f_{\rho_1\eta_1}&=-\frac{k_BT\bar{\eta}_0}{2\rho_0}\Lambda'(\bar{\eta}_0)+\tfrac{1}{2}\tilde{V}_{31}\ , \end{aligned} \tag{2.24}$$

where $\bar{\eta}_0\equiv\eta_0^{(N)}/\rho_0$ is the mean reduced order parameter in the nematic phase, while $\Lambda'(\bar{\eta}_0)=d\Lambda(\bar{\eta}_0)/d\bar{\eta}_0$. The quantity $\tilde{c}_{\rm HS}(q^*)$ in the first line of (2.24) is the Fourier transform of the hard-sphere direct correlation function in a uniform phase, evaluated at the *scaled*[19,20] wave number $q^*\equiv q\sigma_\parallel/\sigma$ (see the Appendix).

As is well known, (2.22) predicts that a second-order nematic-smectic transition occurs when $c_2=0$, provided that both $c_4>0$ and no other local minima in the full free energy preempt that transition. If $c_4<0$, then the vanishing of c_2 describes a supercooling spinodal line for the nematic phase, the true (first-order) transition from nematic to smectic having occurred at some higher temperature where c_2 is still positive. Even in the latter cases, we have found (see Sec. III) that the locus $c_2=0$ is generally quite close to the nematic-smectic phase boundary, and so provides a useful method of estimating that boundary for different molecular parameters. The simultaneous vanishing of c_4 determines, at least for all cases we have studied, the location of the tricritical point[30,31] separating first-order from second-order N–Sm-A transitions.

It is straightforward to calculate the "critical temperature" $T_c(\rho_0;d)$ at a given mean density and period which satisfies the condition $c_2=0$, using the expressions in (2.23) and (2.24) and the equilibrium condition for the order parameter of the reference nematic state:

$$k_BT\Lambda(\bar{\eta}_0)+\tilde{V}_{20}\rho_0\bar{\eta}_0=0\ . \tag{2.25}$$

Under conditions that the nematic state is locally stable, i.e., the second derivative $f_{\eta_0\eta_0}$ with respect to η_0 is positive, it can be shown[32] that the function $f_{\eta_1\eta_1}$ is also positive and so does not lead to a singularity in the expression (2.23) for c_2. Similar to Ref. 12(a), we consider the physically relevant critical temperature to be $T_c(\rho_0)=\max_d T_c(\rho_0;d)$, i.e., maximized with respect to $d=2\pi/q$. Having determined $T_c(\rho_0)$, the sign of the coefficient c_4 can be evaluated to establish the order of the transition. Results are described in Sec. III.

III. RESULTS

We have modeled the components $V_n(r)$, $n=1-3$, of the attractive potential (2.7) by the following Lennard-Jones forms, suggested by the Weeks-Chandler-Andersen[33] treatment of simple fluids:

$$V_n(r)=\begin{cases}\epsilon_n\left[\left(\dfrac{\sigma_n}{r}\right)^{12}-\left(\dfrac{\sigma_n}{r}\right)^{6}\right], & r\geq 2^{1/6}\sigma_n\\ -\epsilon_n/4, & r<2^{1/6}\sigma_n\ .\end{cases} \tag{3.1}$$

Clearly, these are rather arbitrary choices whose only real claim to reality is the power-law decay $\propto r^{-6}$ at large distances, appropriate for dispersion interactions.[23] We can let the parameter ϵ_1 (>0) be arbitrary, as this merely sets the temperature scale. Following Ref. 13, we have fixed the ratio $\epsilon_2/\epsilon_1=0.3$, which is expected to be typical of real liquid crystals. In the absence of a detailed knowledge of the functions $V_n(r)$, it is reasonable to choose the range parameters to be equal, i.e., $\sigma_3=\sigma_2=\sigma_1$. Given that those functions represent leading-order spherical-harmonic expansion coefficients of the potential $V_A(1,2)$,[18] we expect values of the σ_n to be on the order of an angle-averaged molecular diameter, i.e., comparable to the equivalent hard-sphere diameter σ. However, without loss of generality, we can *choose* $\sigma_1=\sigma$, since any difference between the latter parameters can be absorbed by suitable rescaling of ϵ_1 and the anisotropy ratio $\sigma_\parallel/\sigma$. In the following, all distances are ex-

pressed in units of σ and likewise all densities in units of σ^{-3}.

Here we examine the behavior predicted by the theory as $\sigma_\parallel/\sigma$ and the relative strength ϵ_3/ϵ_1 of the symmetry-breaking potential $V_3(r)$ vary. These parameters affect only the properties of modulated phases in the theory, while the behavior of nematic and isotropic fluids are the same as described in Ref. 13. We take ϵ_3 to be negative, since this results [cf. (2.7) and (3.1)] in a greater attractive energy between two parallel molecules in a side-by-side relative to an end-to-end configuration, an expected property of rod-shaped molecules.[18]

Many qualitative features of the theory can be understood by examining the wave-number dependence of the Fourier transforms $\tilde{V}_n(q)$ and $\tilde{c}_{\rm HS}(q^*)$. The former were evaluated from (2.19) and (3.1), using integration by parts to express $\tilde{V}_n(q)$ in terms of elementary functions and the sine integral.[34] Examples are shown in Figs. 1 and 2, where q is given in units of σ^{-1}. The functions $\tilde{V}_1(q)$ and $\tilde{V}_2(q)$ both exhibit a global minimum at $q=0$, while weakly oscillating about zero at large wave number. The function $\tilde{V}_3(q)$ vanishes at $q=0$, as noted earlier, then exhibits a broad minimum followed by weaker oscillations. In contrast, the modified direct correlation function $1/\rho_0-\tilde{c}_{\rm HS}(q^*)\equiv\hat{c}_{\rm HS}(q^*)$ has an absolute maximum at $q=0$ (proportional to the hard-sphere inverse compressibility) and a weak global minimum at a q^* in the range $6\le q^*\le 7$ which, as indicated in Fig. 2, increases with density.

Let us examine the implications of these features for the Landau coefficient c_2 obtained from (2.23) and (2.24). Considering first the contribution of the function $f_{\rho_1\rho_1}$, it is clear that the behavior of this function for small q is governed by the opposing behaviors of $\tilde{V}_{11}\equiv\tilde{V}_1(q)$ and $\hat{c}_{\rm HS}(q^*)$. We have found that $\hat{c}_{\rm HS}(q^*)$ at its minimum becomes negative for mean densities $\rho_0\gtrsim 1.2$. In the absence of all attractive contributions, that would lead to a negative c_2 and hence instability of the isotropic hard-sphere or aligned hard-ellipsoid fluid to a one-dimensionally modulated phase only at densities $\rho_0\gtrsim 1.2$. However, three-dimensional crystallization occurs in such a fluid at much lower mean densities [$\rho_0\approx 0.94$ (Refs. 16 and 20)], so we conclude that the model without attractive interactions does not produce a stable smectic phase. On the other hand, in the *absence* of $\hat{c}_{\rm HS}(q^*)$, the function $\tilde{V}_1(q)$ would produce a global minimum in $f_{\rho_1\rho_1}$ and hence in c_2 at $q=0$, i.e., at *infinite* period d. It can be seen from (2.23), (2.24) and Fig. 1 that the latter outcome is not modified by including contributions to c_2 of the functions $f_{\eta_1\eta_1}$ and $f_{\rho_1\eta_1}$. To avoid the unphysical result $q\to 0$ in theories of the McMillan-Kobayashi type,[3–5] which omit explicit hard-core effects, the period has to be inserted "by hand." In the present theory, a nonzero lower limit to the equilibrium wave number follows naturally from the behavior of $\hat{c}_{\rm HS}(q^*)$ shown in Fig. 2. We have found that the equilibrium wave number generally lies close to that corresponding to the minimum of $\hat{c}_{\rm HS}(q^*)$

The relation between the scales of q and q^* is governed by the ratio $\sigma_\parallel/\sigma$. When $\sigma_\parallel/\sigma=1$, i.e., on neglecting anisotropy of the core, Figs. 1 and 2 show that the global minimum of $\hat{c}_{\rm HS}(q^*)$ approximately coincides with the weak *secondary* minima of $\tilde{V}_1(q)$ and $\tilde{V}_2(q)$. As for the case discussed above when $\hat{c}_{\rm HS}(q^*)$ alone operates, we expect that any "smectic" ordering found under these conditions would be preempted by formation of a crystalline solid. When $\sigma_\parallel/\sigma$ is increased to 2,[35] the minimum in $\hat{c}_{\rm HS}(q^*)$ approximately coincides with the relative *maxima* in the functions $\tilde{V}_1(q)$ and $\tilde{V}_2(q)$. While the positive values of the latter functions would now tend to oppose smectic formation, these are compensated by the negative well in $\tilde{V}_3(q)$. Therefore, under these conditions, the "symmetry-breaking" potential $V_3(r)$ should play a crucial role in stabilizing the smectic state, as will be seen below.

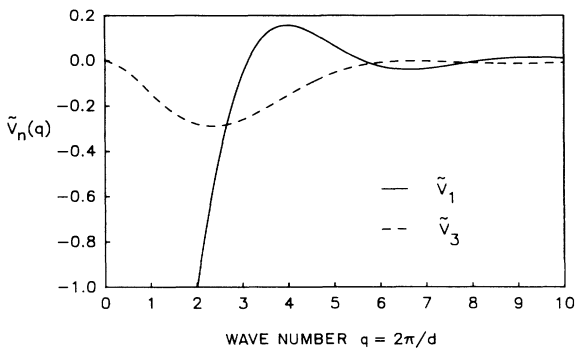

FIG. 1. Fourier transforms $\tilde{V}_n(q)$ of the components of the attractive pair potential, in units of $\epsilon_1\sigma^3$, for $|\epsilon_3/\epsilon_1|=0.34$. The function $\tilde{V}_2(q)$ is not shown, as this is identical to $\tilde{V}_1(q)$ with amplitude scaled by ϵ_2/ϵ_1.

Let us now turn to the predictions of the full model. Representative phase diagrams are shown in Figs. 3–6. In contrast to previous theories of smectic liquid crystals, with the exception of Refs. 10 and 12, two independent thermodynamic variables enter the present description, namely, temperature and density (Figs. 3 and 4) or temperature and pressure (Figs. 5 and 6). Here the reduced units for temperature and pressure are $T^*\equiv k_BT/\epsilon_1$ and $P^*\equiv P\sigma^3/\epsilon_1$. The results in Figs. 3–6 have been obtained for a fixed value $\sigma_\parallel/\sigma=1.8$, while the relative strength parameter $|\epsilon_3/\epsilon_1|$ equals 0.28 (Figs. 3 and 5) and

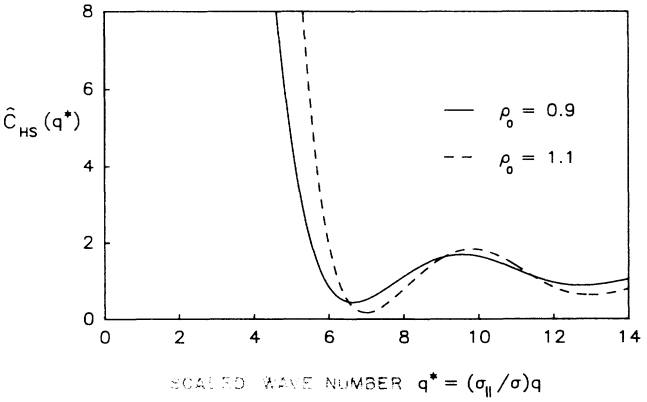

FIG. 2. Fourier transform of the modified direct correlation function for a hard-sphere fluid, $\hat{c}_{\rm HS}(q^*)\equiv 1/\rho_0-\tilde{c}_{\rm HS}(q^*)$.

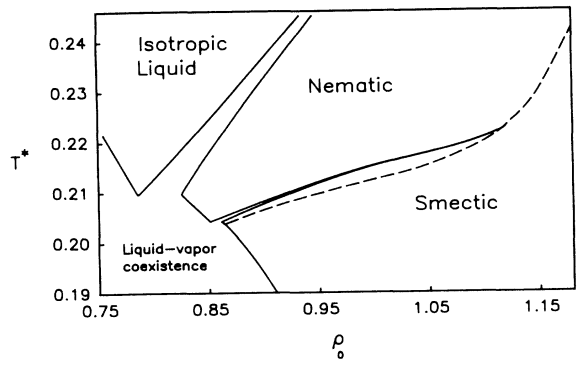

FIG. 3. Temperature-density phase diagram at $\sigma_{\parallel}/\sigma=1.8$, $|\epsilon_3/\epsilon_1|=0.28$.

0.34 (Figs. 4 and 6). For computational convenience, smectic phase boundaries were calculated using $M=5$ terms in the Fourier series (2.14) for the order parameters. Selected checks indicate that all first-order smectic phase boundaries shown differ by less than 0.5% from those obtained using a much larger number ($M=20$) of Fourier components.

The diagrams show isotropic vapor and liquid as well as nematic and smectic phases, separated by second-order (dashed) or first-order (solid) phase boundaries, where the latter naturally exhibit density gaps. In Figs. 3 and 4, the extension of the dashed lines into the regions of first-order nematic-smectic coexistence represents the spinodal loci determined by vanishing of the Landau coefficient c_2. In the temperature-density plane, the boundary of the condensed phases on the left of the diagram is part of the liquid-vapor coexistence curve, which extends up to the isotropic critical temperature $T^*_{c,\mathrm{LV}}=0.3557$. Although usually ignored in liquid-crystal studies, we see that inclusion of the vapor is significant in establishing limits of thermodynamic stability for the condensed phases. This is also of fundamental interest for several questions concerning interfaces of liquid crystals.[13,14,18] On the other hand, we have not examined the stability of the phases with respect to solid formation, but in view of earlier remarks the latter is expected to preempt much of the phase domains shown in Figs. 3–6. At present, the treatment of solid phases by

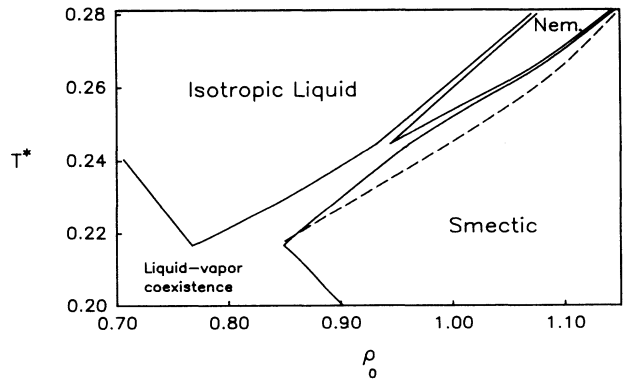

FIG. 4. Temperature-density phase diagram at $\sigma_{\parallel}/\sigma=1.8$, $|\epsilon_3/\epsilon_1|=0.34$.

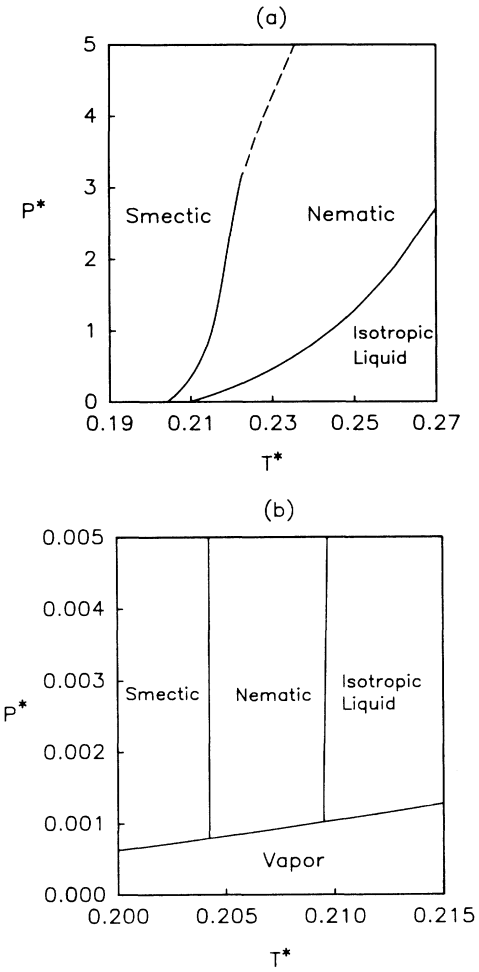

FIG. 5. Pressure-temperature phase diagram corresponding to that in Fig. 3. Part (b) shows the low-pressure region on a magnified scale.

theories similar to the one used here is somewhat problematic when attractive forces are included,[16(a)] and further studies are needed.

At $|\epsilon_3/\epsilon_1|=0.28$, two triple points involving the vapor phase (V) are present, the one at higher T^* due to simultaneous coexistence of the isotropic liquid (I) and nematic (N) phases,[13] that at lower T^* due to coexistence between nematic and smectic (Sm-A) phases. At $|\epsilon_3/\epsilon_1|=0.34$, the stability range of the smectic phase is increased, as expected, and the phase diagrams now exhibit V–I–Sm-A and I–N–Sm-A triple points. As far as we are aware, none of the triple points involving vapor has been directly observed in experiments. Experiments on liquid crystals are usually performed under a fixed atmospheric pressure, although there are several exceptions.[36–38] We estimate[39] that atmospheric pressure corresponds to about $P^*=10^{-4}$ to 10^{-3} in our reduced units, which is comparable with the triple-point vapor pressures shown on Figs. 5 and 6, so that the latter should be within the resolution of experiments. We know of only one instance where a pressure-induced I–N–Sm-A triple point in a pure compound has been observed,[38] although this phenomenon should not be un-

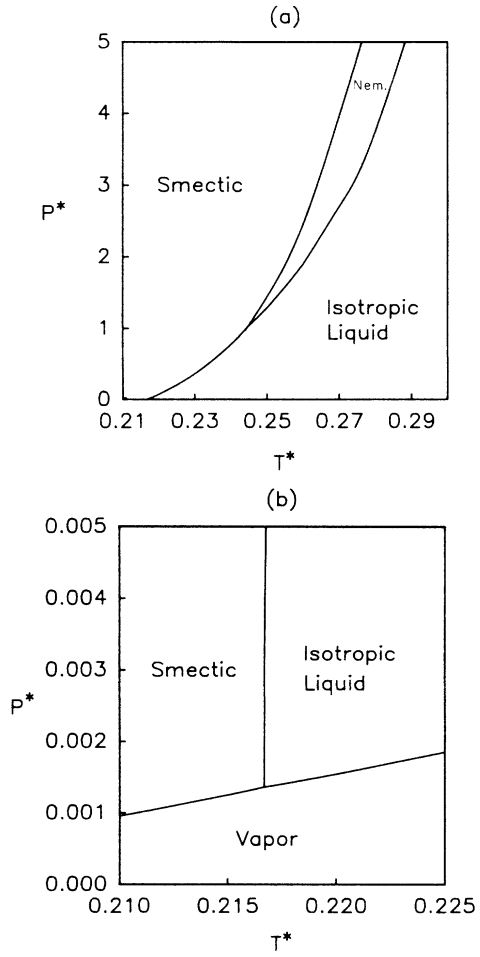

FIG. 6. Pressure-temperature phase diagram corresponding to that in Fig. 4.

common. Data given in Ref. 37 suggest that such a triple point may occur in the cyanobiphenyl series nCB for $n \geq 9$.

The nematic-smectic phase boundaries in Figs. 3–6 are first order over most of the their extent, becoming second order only at very high densities when $|\epsilon_3/\epsilon_1|=0.28$ (where, however, the true stable phase is probably solid). The predominately first-order nature of the nematic-smectic transition disagrees with previous studies based on the McMillan-Kobayashi model, although such studies have usually restricted the Fourier series (2.14) to $M=1$, the limitations of which were first pointed out some time ago by Meyer and Lubensky.[30] We have also found that the range over which the N–Sm-A transition is second order becomes much larger when we truncate the series (2.14) at $M=1$. Additional examples showing the effects of model parameters on the order of the transition are given below.

Another feature of interest is the behavior of the equilibrium smectic period. We find that this is always a decreasing function of density, which is due to the behavior of the minimum of $\hat{c}_{\rm HS}(q^*)$ shown in Fig. 2. In contrast, at fixed density the period weakly decreases when the temperature is increased, as indicated in Fig. 7. Such a

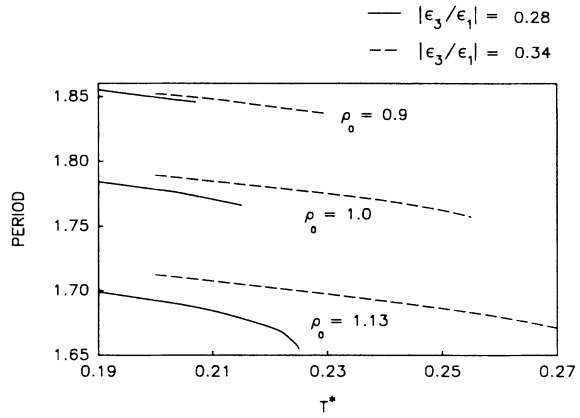

FIG. 7. Variation of the smectic period d with temperature at three different densities, for $\sigma_\parallel/\sigma=1.8$ and at indicated values of $|\epsilon_3/\epsilon_1|$. The high-temperature end points are at the limits of smectic stability. The bottom curve in the figure corresponds to a second-order N–Sm-A transition, while all others correspond to first-order transitions.

tendency has indeed been observed experimentally and previously ascribed to increasing orientational disorder with rise in temperature.[40] Here that phenomenon is more directly related to the competition between repulsive and attractive interactions in our model, as discussed earlier in this section, but we do rule out the previous explanation.[40] That would apply if we generalize the model as described briefly in Sec. II A and account for dependence of the effective diameters $\sigma_\parallel$ and σ on the degree of orientational order.

We close this section by indicating in more detail the effects on phase behavior due to variations in the parameters $\sigma_\parallel/\sigma$ and ϵ_3/ϵ_1. Results are shown in Figs. 8 and 9, where for simplicity we have plotted only the spinodal (or second-order) loci $T_c(\rho_0)$ determined by $c_2=0$. A striking feature of Fig. 8 is the nonmonotonic variation in smectic stability with $\sigma_\parallel/\sigma$ at fixed ϵ_3/ϵ_1, and especially the *decrease* in transition temperature with increasing $\sigma_\parallel/\sigma$ when the latter is near unity. This again can be rationalized in terms of the opposing effects of attractive and repulsive forces. There is also seen to be a qualitative difference between the curves with small ($\lesssim 1.5$) and large values of $\sigma_\parallel/\sigma$. In particular, the transition temperatures in the former cases are more rapidly increasing functions of density. Comparison with Figs. 3 and 4 shows that these will intersect the I-N transition line and thus lead at higher densities to direct transitions between the isotropic liquid and a one-dimensionally modulated "plastic" phase with very weak orientational order. [The orientational order in the latter phase vanishes identically only if the interaction term $V_3(r)$ is zero.] As discussed earlier in this section, we expect these transitions to be unstable relative to solid formation. Figure 8 clearly shows the role of large core anisotropies $\sigma_\parallel/\sigma$ in stabilizing smectic formation at lower densities, where solid phases may not be stable. Note also the unusual behavior of $T_c(\rho_0)$ at $\sigma_\parallel/\sigma=1.7$, in terms of both the reentrant nature of the second-order N–Sm-A transition and the fact that $T_c(\rho_0)$ *decreases* with density over a wide region.

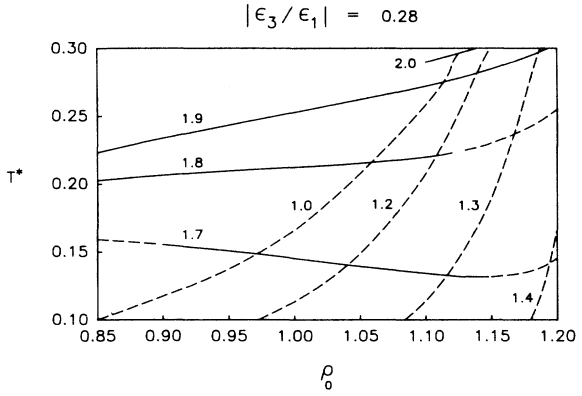

FIG. 8. Smectic-nematic transition lines at different values of $\sigma_\parallel/\sigma$ (labeling the curves), for $|\epsilon_3/\epsilon_1|=0.28$. Spinodal lines and second-order transition lines are drawn as solid and dashed curves, respectively.

Features similar to the latter have been observed in some experiments.[36] This behavior is also shown by some cases in Fig. 9, where $\sigma_\parallel/\sigma$ is fixed at 2 and the ratio $|\epsilon_3/\epsilon_1|$ varies. In this figure the *low-density* boundaries of the curves at $|\epsilon_3/\epsilon_1|=0.20$ and 0.24 (as well as at $|\epsilon_3/\epsilon_1|=0.28$ and $\sigma_\parallel/\sigma=2$ in Fig. 8) correspond to the limits of nematic stability. At lower densities, these give way to isotropic-smectic transitions such as seen in Fig. 4. The decrease in smectic stability with decreasing magnitude of $|\epsilon_3/\epsilon_1|$ is quite apparent in Fig. 9. The small domain of smectic formation indicated when $\epsilon_3=0$ is not realizable, as this is entirely enclosed by the liquid (nematic)–vapor coexistence region.

IV. DISCUSSION

In the theory presented here, formation of a smectic-A phase results from coupling of repulsive and attractive forces between rod-shaped molecules. On the one hand, we have shown that the theory is consistent with the fact that one-dimensionally modulated phases of parallel ellipsoids must be unstable with respect to crystalline solid phases.[20] (Although this should hold in an exact theory, it is not necessarily satisfied by approximate density-functional theories.) On the other hand, we have given evidence, albeit not proved conclusively, that any smectic

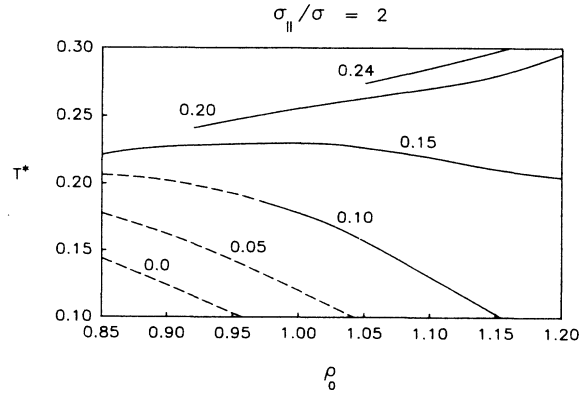

FIG. 9. Similar to Fig. 8, but at different values of $|\epsilon_3/\epsilon_1|$ (labeling the curves), for $\sigma_\parallel/\sigma=2$.

phases apparently induced by anisotropic attractive interactions with *weakly* anisotropic cores ($\sigma_\parallel/\sigma\approx 1$) are also unstable relative to solid phases. Only when the core anisotropy $\sigma_\parallel/\sigma$ *and* the relative strength $|\epsilon_3/\epsilon_1|$ of the symmetry-breaking attractive component $V_3(r)$ are simultaneously large do smectic phases occur under thermal conditions which may not favor solid formation. The theory also shows explicitly how incompressibility of the hard cores determines the equilibrium smectic period d, a quantity which is arbitrarily prescribed in theories of the McMillan-Kobayashi type.[3–5]

A feature missing from the present theory is the occurrence of smectic ordering due to hard-core interactions alone, such as shown by recent computer simulations[6] and density-functional theories[7–9] of hard cylinders and spherocylinders. These works clearly demonstrate that the appearance of smectic ordering is sensitive to the details of molecular shape, given the absence of such ordering for hard ellipsoids. However, apart from simulations in Ref. 6(b), the above studies have considered only systems under the constraint of perfect parallel alignment. *(Note added in proof.* This constraint has been relaxed in recent work by Poniewierski and Holyst,[41] using a density-functional theory similar to the ones described here and in Ref. 9.) While it is found that relaxation of that constraint does not destroy smectic ordering of hard spherocylinders,[6(b)] it is plausible that sensitivity to the precise shape of the core becomes less severe when some orientational disorder is present. One can argue heuristically (but with some support from perturbative arguments[18,9]) that fluctuations in alignment of rigid rod-shaped molecules produce an "effective" repulsive core which is roughly ellipsoidal in shape. Allowing for dependence of the core-shape parameters on the degree of orientational order, the present theory could be extended to accommodate a variety of molecular shapes. Such an extension will be examined in future work. We note that on generalizing the equivalent hard-sphere diameter σ to be a functional of $\hat{f}(z\omega)$, core interactions will also influence the nematic-isotropic phase boundaries,[18] an effect not present here.

The density-functional theory developed in this paper can be generalized to discuss interfaces between the various isotropic and liquid-crystalline phases. This is especially relevant to liquid-vapor interfaces involving the smectic-A phase, which have been modeled in previous work[42] using an impenetrable wall in place of the coexisting vapor. This application will also be considered in future work.

ACKNOWLEDGMENTS

The authors wish to thank A. M. Somoza, P. Tarazona, B. Tjipto-Margo, and M. Lipkin for many useful suggestions and critical remarks, and the first two for providing a preprint of Ref. 9. L. Mederos is grateful to the NATO Scientific Committee for financial support. A grant from the National Sciences and Engineering Research Council (Canada) is also gratefully acknowledged.

APPENDIX

Here we summarize several results related to the averaged density $\bar{\rho}(\mathbf{r})$ defined in (2.5). In the following, all densities are dimensionless and given in units of σ^{-3}. We use the semiempirical model developed by Tarazona,[16(b)] which expresses the dimensionless weighting function $w(s;\bar{\rho})$ in (2.5) as a quadratic expansion in $\bar{\rho}$:

$$w(s;\bar{\rho})=w_0(s)+w_1(s)\bar{\rho}+w_2(s)\bar{\rho}^2 . \tag{A1}$$

The functions $w_0(s)$ and $w_2(s)$ are given by[16(b)]

$$\begin{aligned} w_0(s)&=\frac{3}{4\pi}\Theta(1-s) , \\ w_2(s)&=\frac{5\pi}{144}(6-12s+5s^2)\Theta(1-s) , \end{aligned} \tag{A2}$$

where $\Theta(t)$ is the unit step function. An analytical expression is available for the Fourier transform $\tilde{w}_1(k)$, where in general (for dimensionless wave number k)

$$\tilde{w}_n(k)=\frac{4\pi}{k}\int_0^\infty ds\, s w_n(s)\sin(ks) . \tag{A3}$$

We have

$$\tilde{w}_1(k)=\frac{\tilde{f}(k)-\frac{10\pi}{3}\tilde{w}_0(k)-\frac{5\pi}{3}\tilde{w}_0^2(k)}{8[1+\tilde{w}_0(k)]} , \tag{A4}$$

where

$$\tilde{f}(k)=-\frac{4\pi}{k^2}\left[\left(\frac{5}{2}+\frac{6}{k^2}+\frac{12}{k^4}\right)\cos k+\left(\frac{2}{k}+\frac{12}{k^3}\right)\sin k -12\left(\frac{1}{k^2}+\frac{1}{k^4}\right)\right] . \tag{A5}$$

Inserting (A1) into (2.5), a quadratic equation is obtained for $\bar{\rho}(\mathbf{r})$, which has the physical solution[16(b)]

$$\bar{\rho}(\mathbf{r})=\frac{2\bar{\rho}_0}{1-\bar{\rho}_1+[(1-\bar{\rho}_1)^2-4\bar{\rho}_0\bar{\rho}_2]^{1/2}} , \tag{A6}$$

where $\bar{\rho}_n\equiv\bar{\rho}_n(\mathbf{r})$ is defined as

$$\bar{\rho}_n\equiv\bar{\rho}_n(\mathbf{r})=\int d\mathbf{s}\, w_n(s)\rho(\mathbf{r}+\vec{\sigma}\cdot\mathbf{s}) . \tag{A7}$$

We note that when $\rho(\mathbf{r})=\rho(z)$ varies only as a function of z, only the eigenvalue $\sigma_\parallel$ of the tensor $\vec{\sigma}$ defined below (2.5) is relevant. Using the Fourier representation for $\rho(z)$ in (2.14), the last equation then gives

$$\bar{\rho}_n(z)=\sum_{m=0}^{M}\rho_m\tilde{w}_n(mq\sigma_\parallel)\cos(mqz) . \tag{A8}$$

For completeness, we list the expressions for $\tilde{w}_0(k)$ and $\tilde{w}_2(k)$ obtained from (A2) and (A3):

$$\begin{aligned} \tilde{w}_0(k)&=\frac{3}{k^3}(\sin k-k\cos k) , \\ \tilde{w}_2(k)&=\frac{5\pi^2}{36k^2}\left[\left[1+\frac{6}{k^2}\right]\cos k -\left[\frac{3}{k}+\frac{30}{k^3}\right]\sin k+\frac{24}{k^2}\right] . \end{aligned} \tag{A9}$$

The limits of these at vanishing k are $\tilde{w}_0(k=0)=1$, $\tilde{w}_n(k=0)=0$ for $n=1,2$.

From a calculation discussed in Ref. 16(b), the Fourier transform of the direct correlation function for an isotropic hard-sphere fluid of mean density ρ_0 and molecular diameter σ is, in units of σ^3,

$$\tilde{c}_{\rm HS}(q)=-2\Delta\psi'_{\rm HS}(\rho_0)\tilde{w}(q\sigma)-\rho_0\Delta\psi''_{\rm HS}(\rho_0)\tilde{w}^2(q\sigma) -2\rho_0\Delta\psi'_{\rm HS}(\rho_0)\tilde{w}(q\sigma)\tilde{w}'(q\sigma) , \tag{A10}$$

where $\Delta\psi'_{\rm HS}(\rho_0)$ and $\Delta\psi''_{\rm HS}(\rho_0)$ denote the first and second derivatives, respectively, of the excess free energy (2.6) with respect to ρ_0. Here

$$\begin{aligned} \tilde{w}(k)&=\tilde{w}_0(k)+\rho_0\tilde{w}_1(k)+\rho_0^2\tilde{w}_2(k) , \\ \tilde{w}'(k)&=\tilde{w}_1(k)+2\rho_0\tilde{w}_2(k) . \end{aligned} \tag{A11}$$

As all correlations in the modulated phase involve the dimensionless wave number $q\sigma_\parallel$, cf. (A8), we can view these as obtained from corresponding hard-sphere quantities on evaluating the latter with the scaled wave number $q^*=(\sigma_\parallel/\sigma)q$.

---

*Permanent address: Instituto de Ciencia de Materiales (CSIC) and Departamento de Fisica de la Materia Condensada, Universidad Autonoma de Madrid, E-28049 Madrid, Spain.

[1](a) B. A. Baron and W. M. Gelbart, J. Chem. Phys. **67**, 5795 (1977); (b) W. M. Gelbart and B. Barboy, Mol. Cryst. Liq. Cryst. **55**, 209 (1979).

[2]M. A. Cotter, J. Chem. Phys. **66**, 1098 (1977).

[3]W. L. McMillan, Phys. Rev. A **4**, 1238 (1971); **6**, 936 (1972).

[4]K. K. Kobayashi, J. Phys. Soc. Jpn. **29**, 101 (1970); Mol. Cryst. Liq. Cryst. **13**, 137 (1971).

[5]Selected articles based on the McMillan-Kobayashi approach are F. T. Lee, H. T. Tan, Y. M. Shih and C.-W. Woo, Phys. Rev. Lett. **18**, 1117 (1973); P. J. Photinos and A. Saupe, Phys. Rev. A **13**, 1926 (1976); M. R. Kuzma and D. W. Allender, *ibid.* **25**, 2793 (1982); G. R. Kventsel, G. F. Luckhurst, and H. B. Zewdie, Mol. Phys. **56**, 589 (1985).

[6](a) A. Stroobants, H. N. W. Lekkerkerker, and D. Frenkel, Phys. Rev. Lett. **57**, 1452 (1986); Phys. Rev. A **36**, 2929 (1987); (b) D. Frenkel, J. Phys. Chem. **92**, 3280 (1988).

[7]B. Mulder, Phys. Rev. A **35**, 3095 (1987).

[8]X. Wen and R. B. Meyer, Phys. Rev. Lett. **59**, 1325 (1987).

[9]A. M. Somoza and P. Tarazona (unpublished).

[10]M. Hosino, H. Nakano, and H. Kimura, J. Phys. Soc. Jpn. **50**, 1067 (1981).

[11]M. Nakagawa and T. Akahane, J. Phys. Soc. Jpn. **53**, 1951 (1984).

[12](a) J. Stecki and A. Kloczkowski, Mol. Phys. **42**, 51 (1981); (b) A. Kloczkowski and J. Stecki, *ibid.* **55**, 689 (1985).

[13]M. M. Telo da Gama, Mol. Phys. **52**, 585 (1984).

[14]J. H. Thurtell, M. M. Telo da Gama, and K. E. Gubbins, Mol. Phys. **54**, 321 (1985).

[15]P. Tarazona and R. Evans, Mol. Phys. **52**, 847 (1984).

[16](a) P. Tarazona, Mol. Phys. **52**, 81 (1984); (b) Phys. Rev. A **31**, 2672 (1985); P. Tarazona, U. Marini Bettolo Marconi, and R. Evans, Mol. Phys. **60**, 573 (1987).

[17]L. Mederos, P. Tarazona, and G. Navascués, Phys. Rev. B **35**, 3376 (1987); **35**, 3384 (1987).

[18]B. Tjipto-Margo and D. E. Sullivan, J. Chem. Phys. **88**, 6620 (1988); B. Tjipto-Margo, Ph.D. thesis, University of Guelph, 1988.

[19]J. L. Lebowitz and J. W. Perram, Mol. Phys. **50**, 1207 (1983).

[20]P. Harrowell and D. W. Oxtoby, Mol. Phys. **54**, 1325 (1985).

[21]H. Schröder, Ber. Bunsenges. Phys. Chem. **78**, 855 (1974); L. Senbetu and C.-W. Woo, Phys. Rev. A **17**, 1529 (1978).

[22]M. D. Lipkin and D. W. Oxtoby, J. Chem. Phys. **79**, 1939 (1983).

[23]C. G. Gray and K. E. Gubbins, *Theory of Molecular Fluids* (Clarendon, Oxford, England, 1984).

[24]An alternative method for including partial orientational order has been proposed in Ref. 9. The scaling ideas used in the latter reference are similar to those discussed here.

[25]Related approaches using a "coarse-grained" density have been described by T. F. Meister and D. M. Kroll, Phys. Rev. A **31**, 4055 (1985); W. A. Curtin and N. W. Ashcroft, *ibid.* **32**, 2909 (1985); Phys. Rev. Lett. **56**, 2775 (1986).

[26]W. Maier and A. Saupe, Z. Naturforsch. **13A**, 564 (1958); **14A**, 882 (1959); **15A**, 287 (1960).

[27]D. Ronis and C. Rosenblatt, Phys. Rev. A **21**, 1687 (1980); C. Rosenblatt and D. Ronis, *ibid.* **23**, 305 (1981); Y. Drossinos and D. Ronis, *ibid.* **33**, 589 (1986).

[28]W. H. Press, B. P. Flannery, S. A. Teukolsky, and W. T. Vetterling, *Numerical Recipes: The Art of Scientific Computing* (Cambridge University Press, Cambridge, England, 1986).

[29]P. G. de Gennes, *The Physics of Liquid Crystals* (Clarendon, Oxford, England, 1975).

[30]R. B. Meyer and T. C. Lubensky, Phys. Rev. A **14**, 2307 (1976).

[31]L. Longa, J. Chem. Phys. **85**, 2974 (1986).

[32]It is easily shown that $f_{\eta_1\eta_1} > \frac{1}{2} f_{\eta_0\eta_0}$, hence $f_{\eta_1\eta_1} > 0$, from the fact that $\tilde{V}_2(q) > \tilde{V}_2(0)$ for any nonzero q, as discussed in Sec. III.

[33]J. D. Weeks, D. Chandler, and H. C. Andersen, J. Chem. Phys. **54**, 5237 (1971).

[34]*Handbook of Mathematical Functions*, edited by M. Abramowitz and I. A. Stegun (Dover, New York, 1972).

[35]Recalling that $\sigma = (\sigma_\perp^2 \sigma_\parallel)^{1/3}$, hence $\sigma_\parallel/\sigma = (\sigma_\parallel/\sigma_\perp)^{2/3}$, one sees that the value $\sigma_\parallel/\sigma = 2$ implies a length-to-breadth ratio $\sigma_\parallel/\sigma_\perp \approx 2.83$, approaching values typical of mesogenic molecules.

[36]P. H. Keyes, H. T. Weston, W. J. Lin, and W. B. Daniels, J. Chem. Phys. **63**, 5006 (1975).

[37]R. Shashidar and G. Venkatesh, J. Phys. (Paris) Colloq. **40**, C3-396 (1979).

[38]P. E. Cladis, D. Guillon, W. B. Daniels, and A. C. Griffin, Mol. Cryst. Liq. Cryst. **56**, 89 (1979).

[39]Estimates of molecular volumes typically give $\sigma^3 \approx 500 A^3$ [Ref. 1(a)]. The average well depth $\epsilon_1/4$ of intermolecular forces is more uncertain, but is expected to be on the order of 10^{-13} to 10^{-12} erg (Refs. 1, 2, and 13). Thus we estimate ϵ_1/σ^3 to be in the range 10^9 to 10^{10} erg cm^{-3} (≈ 1 to 10 kbar).

[40]A. de Vries, J. Chem. Phys. **71**, 25 (1979); Mol. Cryst. Liq. Cryst. **131**, 125 (1985).

[41]A. Poniewierski and R. Holyst (unpublished).

[42]Z. Pawloska, G. F. Kventsel, and T. J. Sluckin, Phys. Rev. A **36**, 992 (1987); J. V. Selinger and D. Nelson, *ibid.* **37**, 1736 (1988).